PHYSICAL REVIEW D **76,** 111104(R) (2007)

Measurement of the $p\bar{p} \to WZ + X$ cross section at $\sqrt{s} = 1.96$ TeV and limits on WWZ trilinear gauge couplings

V. M. Abazov,[35] B. Abbott,[75] M. Abolins,[65] B. S. Acharya,[28] M. Adams,[51] T. Adams,[49] E. Aguilo,[5] S. H. Ahn,[30] M. Ahsan,[59] G. D. Alexeev,[35] G. Alkhazov,[39] A. Alton,[64,*] G. Alverson,[63] G. A. Alves,[2] M. Anastasoaie,[34] L. S. Ancu,[34] T. Andeen,[53] S. Anderson,[45] B. Andrieu,[16] M. S. Anzelc,[53] Y. Arnoud,[13] M. Arov,[60] M. Arthaud,[17] A. Askew,[49] B. Åsman,[40] A. C. S. Assis Jesus,[3] O. Atramentov,[49] C. Autermann,[20] C. Avila,[7] C. Ay,[23] F. Badaud,[12] A. Baden,[61] L. Bagby,[52] B. Baldin,[50] D. V. Bandurin,[59] S. Banerjee,[28] P. Banerjee,[28] E. Barberis,[63] A.-F. Barfuss,[14] P. Bargassa,[80] P. Baringer,[58] J. Barreto,[2] J. F. Bartlett,[50] U. Bassler,[16] D. Bauer,[43] S. Beale,[5] A. Bean,[58] M. Begalli,[3] M. Begel,[71] C. Belanger-Champagne,[40] L. Bellantoni,[50] A. Bellavance,[50] J. A. Benitez,[65] S. B. Beri,[26] G. Bernardi,[16] R. Bernhard,[22] L. Berntzon,[14] I. Bertram,[42] M. Besançon,[17] R. Beuselinck,[43] V. A. Bezzubov,[38] P. C. Bhat,[50] V. Bhatnagar,[26] C. Biscarat,[19] G. Blazey,[52] F. Blekman,[43] S. Blessing,[49] D. Bloch,[18] K. Bloom,[67] A. Boehnlein,[50] D. Boline,[62] T. A. Bolton,[59] G. Borissov,[42] T. Bose,[77] A. Brandt,[78] R. Brock,[65] G. Brooijmans,[70] A. Bross,[50] D. Brown,[81] N. J. Buchanan,[49] D. Buchholz,[53] M. Buehler,[81] V. Buescher,[21] S. Bunichev,[37] S. Burdin,[42,†] S. Burke,[45] T. H. Burnett,[82] C. P. Buszello,[43] J. M. Butler,[62] P. Calfayan,[24] S. Calvet,[14] J. Cammin,[71] W. Carvalho,[3] B. C. K. Casey,[77] N. M. Cason,[55] H. Castilla-Valdez,[32] S. Chakrabarti,[17] D. Chakraborty,[52] K. M. Chan,[55] K. Chan,[5] A. Chandra,[48] F. Charles,[18,††] E. Cheu,[45] F. Chevallier,[13] D. K. Cho,[62] S. Choi,[31] B. Choudhary,[27] L. Christofek,[77] T. Christoudias,[43,**] S. Cihangir,[50] D. Claes,[67] B. Clément,[18] Y. Coadou,[5] M. Cooke,[80] W. E. Cooper,[50] M. Corcoran,[80] F. Couderc,[17] M.-C. Cousinou,[14] S. Crépé-Renaudin,[13] D. Cutts,[77] M. Ćwiok,[29] H. da Motta,[2] A. Das,[62] G. Davies,[43] K. De,[78] S. J. de Jong,[34] E. De La Cruz-Burelo,[64] C. De Oliveira Martins,[3] J. D. Degenhardt,[64] F. Déliot,[17] M. Demarteau,[50] R. Demina,[71] D. Denisov,[50] S. P. Denisov,[38] S. Desai,[50] H. T. Diehl,[50] M. Diesburg,[50] A. Dominguez,[67] H. Dong,[72] L. V. Dudko,[37] L. Duflot,[15] S. R. Dugad,[28] D. Duggan,[49] A. Duperrin,[14] J. Dyer,[65] A. Dyshkant,[52] M. Eads,[67] D. Edmunds,[65] J. Ellison,[48] V. D. Elvira,[50] Y. Enari,[77] S. Eno,[61] P. Ermolov,[37] H. Evans,[54] A. Evdokimov,[73] V. N. Evdokimov,[38] A. V. Ferapontov,[59] T. Ferbel,[71] F. Fiedler,[24] F. Filthaut,[34] W. Fisher,[50] H. E. Fisk,[50] M. Ford,[44] M. Fortner,[52] H. Fox,[22] S. Fu,[50] S. Fuess,[50] T. Gadfort,[82] C. F. Galea,[34] E. Gallas,[50] E. Galyaev,[55] C. Garcia,[71] A. Garcia-Bellido,[82] V. Gavrilov,[36] P. Gay,[12] W. Geist,[18] D. Gelé,[18] C. E. Gerber,[51] Y. Gershtein,[49] D. Gillberg,[5] G. Ginther,[71] N. Gollub,[40] B. Gómez,[7] A. Goussiou,[55] P. D. Grannis,[72] H. Greenlee,[50] Z. D. Greenwood,[60] E. M. Gregores,[4] G. Grenier,[19] Ph. Gris,[12] J.-F. Grivaz,[15] A. Grohsjean,[24] S. Grünendahl,[50] M. W. Grünewald,[29] J. Guo,[72] F. Guo,[72] P. Gutierrez,[75] G. Gutierrez,[50] A. Haas,[70] N. J. Hadley,[61] P. Haefner,[24] S. Hagopian,[49] J. Haley,[68] I. Hall,[65] R. E. Hall,[47] L. Han,[6] K. Hanagaki,[50] P. Hansson,[40] K. Harder,[44] A. Harel,[71] R. Harrington,[63] J. M. Hauptman,[57] R. Hauser,[65] J. Hays,[43] T. Hebbeker,[20] D. Hedin,[52] J. G. Hegeman,[33] J. M. Heinmiller,[51] A. P. Heinson,[48] U. Heintz,[62] C. Hensel,[58] K. Herner,[72] G. Hesketh,[63] M. D. Hildreth,[55] R. Hirosky,[81] J. D. Hobbs,[72] B. Hoeneisen,[11] H. Hoeth,[25] M. Hohlfeld,[21] S. J. Hong,[30] S. Hossain,[75] P. Houben,[33] Y. Hu,[72] Z. Hubacek,[9] V. Hynek,[8] I. Iashvili,[69] R. Illingworth,[50] A. S. Ito,[50] S. Jabeen,[62] M. Jaffré,[15] S. Jain,[75] K. Jakobs,[22] C. Jarvis,[61] R. Jesik,[43] K. Johns,[45] C. Johnson,[70] M. Johnson,[50] A. Jonckheere,[50] P. Jonsson,[43] A. Juste,[50] D. Käfer,[20] S. Kahn,[73] E. Kajfasz,[14] A. M. Kalinin,[35] J. R. Kalk,[65] J. M. Kalk,[60] S. Kappler,[20] D. Karmanov,[37] J. Kasper,[62] P. Kasper,[50] I. Katsanos,[70] D. Kau,[49] R. Kaur,[26] V. Kaushik,[78] R. Kehoe,[79] S. Kermiche,[14] N. Khalatyan,[38] A. Khanov,[76] A. Kharchilava,[69] Y. M. Kharzheev,[35] D. Khatidze,[70] H. Kim,[31] T. J. Kim,[30] M. H. Kirby,[34] M. Kirsch,[20] B. Klima,[50] J. M. Kohli,[26] J.-P. Konrath,[22] M. Kopal,[75] V. M. Korablev,[38] A. V. Kozelov,[38] D. Krop,[54] T. Kuhl,[23] A. Kumar,[69] S. Kunori,[61] A. Kupco,[10] T. Kurča,[19] J. Kvita,[8] F. Lacroix,[12] D. Lam,[55] S. Lammers,[70] G. Landsberg,[77] P. Lebrun,[19] W. M. Lee,[50] A. Leflat,[37] F. Lehner,[41] J. Lellouch,[16] J. Leveque,[45] P. Lewis,[43] J. Li,[78] Q. Z. Li,[50] L. Li,[48] S. M. Lietti,[4] J. G. R. Lima,[52] D. Lincoln,[50] J. Linnemann,[65] V. V. Lipaev,[38] R. Lipton,[50] Y. Liu,[6,**] Z. Liu,[5] L. Lobo,[43] A. Lobodenko,[39] M. Lokajicek,[10] A. Lounis,[18] P. Love,[42] H. J. Lubatti,[82] A. L. Lyon,[50] A. K. A. Maciel,[2] D. Mackin,[80] R. J. Madaras,[46] P. Mättig,[25] C. Magass,[20] A. Magerkurth,[64] N. Makovec,[15] P. K. Mal,[55] H. B. Malbouisson,[3] S. Malik,[67] V. L. Malyshev,[35] H. S. Mao,[50] Y. Maravin,[59] B. Martin,[13] R. McCarthy,[72] A. Melnitchouk,[66] A. Mendes,[14] L. Mendoza,[7] P. G. Mercadante,[4] M. Merkin,[37] K. W. Merritt,[50] J. Meyer,[21] A. Meyer,[20] M. Michaut,[17] T. Millet,[19] J. Mitrevski,[70] J. Molina,[3] R. K. Mommsen,[44] N. K. Mondal,[28] R. W. Moore,[5] T. Moulik,[58] G. S. Muanza,[19] M. Mulders,[50] M. Mulhearn,[70] O. Mundal,[21] L. Mundim,[3] E. Nagy,[14] M. Naimuddin,[50] M. Narain,[77] N. A. Naumann,[34] H. A. Neal,[64] J. P. Negret,[7] P. Neustroev,[39] H. Nilsen,[22] H. Nogima,[3] A. Nomerotski,[50] S. F. Novaes,[4] T. Nunnemann,[24] V. O'Dell,[50] D. C. O'Neil,[5] G. Obrant,[39] C. Ochando,[15] D. Onoprienko,[59] N. Oshima,[50] J. Osta,[55] R. Otec,[9] G. J. Otero y Garzón,[51] M. Owen,[44] P. Padley,[80] M. Pangilinan,[77] N. Parashar,[56] S.-J. Park,[71] S. K. Park,[30] J. Parsons,[70] R. Partridge,[77] N. Parua,[54] A. Patwa,[73] G. Pawloski,[80] B. Penning,[22] M. Perfilov,[37] K. Peters,[44] Y. Peters,[25] P. Pétroff,[15] M. Petteni,[43] R. Piegaia,[1] J. Piper,[65]

M.-A. Pleier,[21] P. L. M. Podesta-Lerma,[32,‡] V. M. Podstavkov,[50] Y. Pogorelov,[55] M.-E. Pol,[2] P. Polozov,[36] B. G. Pope,[65] A. V. Popov,[38] C. Potter,[5] W. L. Prado da Silva,[3] H. B. Prosper,[49] S. Protopopescu,[73] J. Qian,[64] A. Quadt,[21,§] B. Quinn,[66] A. Rakitine,[42] M. S. Rangel,[2] K. Ranjan,[27] P. N. Ratoff,[42] P. Renkel,[79] S. Reucroft,[63] P. Rich,[44] M. Rijssenbeek,[72] I. Ripp-Baudot,[18] F. Rizatdinova,[76] S. Robinson,[43] R. F. Rodrigues,[3] M. Rominsky,[75] C. Royon,[17] P. Rubinov,[50] R. Ruchti,[55] G. Safronov,[36] G. Sajot,[13] A. Sánchez-Hernández,[32] M. P. Sanders,[16] A. Santoro,[3] G. Savage,[50] L. Sawyer,[60] T. Scanlon,[43] D. Schaile,[24] R. D. Schamberger,[72] Y. Scheglov,[39] H. Schellman,[53] P. Schieferdecker,[24] T. Schliephake,[25] C. Schwanenberger,[44] A. Schwartzman,[68] R. Schwienhorst,[65] J. Sekaric,[49] H. Severini,[75] E. Shabalina,[51] M. Shamim,[59] V. Shary,[17] A. A. Shchukin,[38] R. K. Shivpuri,[27] D. Shpakov,[50] V. Siccardi,[18] V. Simak,[9] V. Sirotenko,[50] P. Skubic,[75] P. Slattery,[71] D. Smirnov,[55] J. Snow,[74] G. R. Snow,[67] S. Snyder,[73] S. Söldner-Rembold,[44] L. Sonnenschein,[16] A. Sopczak,[42] M. Sosebee,[78] K. Soustruznik,[8] M. Souza,[2] B. Spurlock,[78] J. Stark,[13] J. Steele,[60] V. Stolin,[36] D. A. Stoyanova,[38] J. Strandberg,[64] S. Strandberg,[40] M. A. Strang,[69] M. Strauss,[75] E. Strauss,[72] R. Ströhmer,[24] D. Strom,[53] L. Stutte,[50] S. Sumowidagdo,[49] P. Svoisky,[55] A. Sznajder,[3] M. Talby,[14] P. Tamburello,[45] A. Tanasijczuk,[1] W. Taylor,[5] J. Temple,[45] B. Tiller,[24] F. Tissandier,[12] M. Titov,[17] V. V. Tokmenin,[35] T. Toole,[61] I. Torchiani,[22] T. Trefzger,[23] D. Tsybychev,[72] B. Tuchming,[17] C. Tully,[68] P. M. Tuts,[70] R. Unalan,[65] S. Uvarov,[39] L. Uvarov,[39] S. Uzunyan,[52] B. Vachon,[5] P. J. van den Berg,[33] R. Van Kooten,[54] W. M. van Leeuwen,[33] N. Varelas,[51] E. W. Varnes,[45] I. A. Vasilyev,[38] M. Vaupel,[25] P. Verdier,[19] L. S. Vertogradov,[35] M. Verzocchi,[50] F. Villeneuve-Seguier,[43] P. Vint,[43] P. Vokac,[9] E. Von Toerne,[59] M. Voutilainen,[67,‖] R. Wagner,[68] H. D. Wahl,[49] L. Wang,[61] M. H. L. S Wang,[50] J. Warchol,[55] G. Watts,[82] M. Wayne,[55] M. Weber,[50] G. Weber,[23] A. Wenger,[22,¶] N. Wermes,[21] M. Wetstein,[61] A. White,[78] D. Wicke,[25] G. W. Wilson,[58] S. J. Wimpenny,[48] M. Wobisch,[60] D. R. Wood,[63] T. R. Wyatt,[44] Y. Xie,[77] S. Yacoob,[53] R. Yamada,[50] M. Yan,[61] T. Yasuda,[50] Y. A. Yatsunenko,[35] K. Yip,[73] H. D. Yoo,[77] S. W. Youn,[53] J. Yu,[78] A. Zatserklyaniy,[52] C. Zeitnitz,[25] D. Zhang,[50] T. Zhao,[82] B. Zhou,[64] J. Zhu,[72] M. Zielinski,[71] D. Zieminska,[54] A. Zieminski,[54] L. Zivkovic,[70] V. Zutshi,[52] and E. G. Zverev[37]

(D0 Collaboration)

[1]*Universidad de Buenos Aires, Buenos Aires, Argentina*
[2]*LAFEX, Centro Brasileiro de Pesquisas Físicas, Rio de Janeiro, Brazil*
[3]*Universidade do Estado do Rio de Janeiro, Rio de Janeiro, Brazil*
[4]*Instituto de Física Teórica, Universidade Estadual Paulista, São Paulo, Brazil*
[5]*University of Alberta, Edmonton, Alberta, Canada, Simon Fraser University, Burnaby, British Columbia, Canada, York University, Toronto, Ontario, Canada, and McGill University, Montreal, Quebec, Canada*
[6]*University of Science and Technology of China, Hefei, Peoples Republic of China*
[7]*Universidad de los Andes, Bogotá, Colombia*
[8]*Center for Particle Physics, Charles University, Prague, Czech Republic*
[9]*Czech Technical University, Prague, Czech Republic*
[10]*Center for Particle Physics, Institute of Physics, Academy of Sciences of the Czech Republic, Prague, Czech Republic*
[11]*Universidad San Francisco de Quito, Quito, Ecuador*
[12]*Laboratoire de Physique Corpusculaire, IN2P3-CNRS, Université Blaise Pascal, Clermont-Ferrand, France*
[13]*Laboratoire de Physique Subatomique et de Cosmologie, IN2P3-CNRS, Universite de Grenoble 1, Grenoble, France*
[14]*CPPM, IN2P3-CNRS, Université de la Méditerranée, Marseille, France*
[15]*Laboratoire de l'Accélérateur Linéaire, IN2P3-CNRS et Université Paris-Sud, Orsay, France*
[16]*LPNHE, IN2P3-CNRS, Universités Paris VI and VII, Paris, France*
[17]*DAPNIA/Service de Physique des Particules, CEA, Saclay, France*
[18]*IPHC, Université Louis Pasteur et Université de Haute Alsace, CNRS, IN2P3, Strasbourg, France*
[19]*IPNL, Université Lyon 1, CNRS/IN2P3, Villeurbanne, France and Université de Lyon, Lyon, France*
[20]*III. Physikalisches Institut A, RWTH Aachen, Aachen, Germany*
[21]*Physikalisches Institut, Universität Bonn, Bonn, Germany*
[22]*Physikalisches Institut, Universität Freiburg, Freiburg, Germany*
[23]*Institut für Physik, Universität Mainz, Mainz, Germany*
[24]*Ludwig-Maximilians-Universität München, München, Germany*
[25]*Fachbereich Physik, University of Wuppertal, Wuppertal, Germany*
[26]*Panjab University, Chandigarh, India*
[27]*Delhi University, Delhi, India*
[28]*Tata Institute of Fundamental Research, Mumbai, India*
[29]*University College Dublin, Dublin, Ireland*
[30]*Korea Detector Laboratory, Korea University, Seoul, Korea*
[31]*SungKyunKwan University, Suwon, Korea*
[32]*CINVESTAV, Mexico City, Mexico*

[33]*FOM-Institute NIKHEF and University of Amsterdam/NIKHEF, Amsterdam, The Netherlands*
[34]*Radboud University Nijmegen/NIKHEF, Nijmegen, The Netherlands*
[35]*Joint Institute for Nuclear Research, Dubna, Russia*
[36]*Institute for Theoretical and Experimental Physics, Moscow, Russia*
[37]*Moscow State University, Moscow, Russia*
[38]*Institute for High Energy Physics, Protvino, Russia*
[39]*Petersburg Nuclear Physics Institute, St. Petersburg, Russia*
[40]*Lund University, Lund, Sweden, Royal Institute of Technology and Stockholm University, Stockholm, Sweden, and Uppsala University, Uppsala, Sweden*
[41]*Physik Institut der Universität Zürich, Zürich, Switzerland*
[42]*Lancaster University, Lancaster, United Kingdom*
[43]*Imperial College, London, United Kingdom*
[44]*University of Manchester, Manchester, United Kingdom*
[45]*University of Arizona, Tucson, Arizona 85721, USA*
[46]*Lawrence Berkeley National Laboratory and University of California, Berkeley, California 94720, USA*
[47]*California State University, Fresno, California 93740, USA*
[48]*University of California, Riverside, California 92521, USA*
[49]*Florida State University, Tallahassee, Florida 32306, USA*
[50]*Fermi National Accelerator Laboratory, Batavia, Illinois 60510, USA*
[51]*University of Illinois at Chicago, Chicago, Illinois 60607, USA*
[52]*Northern Illinois University, DeKalb, Illinois 60115, USA*
[53]*Northwestern University, Evanston, Illinois 60208, USA*
[54]*Indiana University, Bloomington, Indiana 47405, USA*
[55]*University of Notre Dame, Notre Dame, Indiana 46556, USA*
[56]*Purdue University Calumet, Hammond, Indiana 46323, USA*
[57]*Iowa State University, Ames, Iowa 50011, USA*
[58]*University of Kansas, Lawrence, Kansas 66045, USA*
[59]*Kansas State University, Manhattan, Kansas 66506, USA*
[60]*Louisiana Tech University, Ruston, Louisiana 71272, USA*
[61]*University of Maryland, College Park, Maryland 20742, USA*
[62]*Boston University, Boston, Massachusetts 02215, USA*
[63]*Northeastern University, Boston, Massachusetts 02115, USA*
[64]*University of Michigan, Ann Arbor, Michigan 48109, USA*
[65]*Michigan State University, East Lansing, Michigan 48824, USA*
[66]*University of Mississippi, University, Mississippi 38677, USA*
[67]*University of Nebraska, Lincoln, Nebraska 68588, USA*
[68]*Princeton University, Princeton, New Jersey 08544, USA*
[69]*State University of New York, Buffalo, New York 14260, USA*
[70]*Columbia University, New York, New York 10027, USA*
[71]*University of Rochester, Rochester, New York 14627, USA*
[72]*State University of New York, Stony Brook, New York 11794, USA*
[73]*Brookhaven National Laboratory, Upton, New York 11973, USA*
[74]*Langston University, Langston, Oklahoma 73050, USA*
[75]*University of Oklahoma, Norman, Oklahoma 73019, USA*
[76]*Oklahoma State University, Stillwater, Oklahoma 74078, USA*
[77]*Brown University, Providence, Rhode Island 02912, USA*
[78]*University of Texas, Arlington, Texas 76019, USA*
[79]*Southern Methodist University, Dallas, Texas 75275, USA*
[80]*Rice University, Houston, Texas 77005, USA*
[81]*University of Virginia, Charlottesville, Virginia 22901, USA*

[*]Visitor from Augustana College, Sioux Falls, SD, USA.
[†]Visitor from The University of Liverpool, Liverpool, United Kingdom
[‡]Visitor from ICN-UNAM, Mexico City, Mexico
[§]Visitor from II. Physikalisches Institut, Georg-August-University Göttingen, Germany
[‖]Visitor from Helsinki Institute of Physics, Helsinki, Finland
[¶]Visitor from Universität Zürich, Zürich, Switzerland
[**]Fermilab International Fellow
[††]Deceased

[82]*University of Washington, Seattle, Washington 98195, USA*

(Received 20 September 2007; published 28 December 2007)

We present measurements of the process $p\bar{p} \to WZ + X \to \ell' \nu_{\ell'} \ell \bar{\ell}$ at $\sqrt{s} = 1.96$ TeV, where ℓ and ℓ' are electrons or muons. Using 1 fb^{-1} of data from the D0 experiment, we observe 13 candidates with an expected background of 4.5 ± 0.6 events and measure a cross section $\sigma(WZ) = 2.7^{+1.7}_{-1.3}$ pb. From the number of observed events and the Z boson transverse momentum distribution, we limit the trilinear WWZ gauge couplings to $-0.17 \leq \lambda_Z \leq 0.21 (\Delta\kappa_Z = 0)$ at the 95% C.L. for a form factor scale $\Lambda = 2$ TeV. Further, assuming that $\Delta g_1^Z = \Delta\kappa_Z$, we find $-0.12 \leq \Delta\kappa_Z \leq 0.29 (\lambda_Z = 0)$ at the 95% C.L. These are the most restrictive limits on the WWZ couplings available to date.

DOI: 10.1103/PhysRevD.76.111104 PACS numbers: 14.70.Fm, 13.40.Em, 13.87.Ce, 14.70.Hp

The $SU(2)_L \times U(1)_Y$ structure of the standard model (SM) Lagrangian requires that the massive electroweak gauge bosons, the W and Z bosons, interact with one another at trilinear and quadrilinear vertices. In the SM, the production cross section for $p\bar{p} \to WZ + X$, $\sigma(WZ)$, depends on the strength of the WWZ coupling, $g_{WWZ} = -e\cot\theta_W$, where e is the positron charge and θ_W is the weak mixing angle. At $\sqrt{s} = 1.96$ TeV, the SM predicts $\sigma_{WZ} = 3.68 \pm 0.25$ pb [1]. Any significant deviation from this prediction would be evidence for new physics.

The WWZ interaction can be parametrized by a generalized effective Lagrangian [2,3] with CP-conserving trilinear gauge coupling parameters (TGCs) g_1^Z, κ_Z, and λ_Z that describe the coupling strengths of the vector bosons to the weak field. The TGCs are commonly presented as deviations from their SM values, i.e. as $\Delta g_1^Z = g_1^Z - 1$, $\Delta\kappa_Z = \kappa_Z - 1$, and λ_Z, where $\lambda_Z = 0$ in the SM. Since tree-level unitarity restricts the anomalous couplings to their SM values at asymptotically high energies, each of the couplings must be parametrized as a form factor, e.g. $\lambda_Z(\hat{s}) = \lambda_Z/(1 + \hat{s}/\Lambda^2)^2]$, where Λ is the form factor scale and $\hat{s}$ is the square of the invariant mass of the WZ system. New physics will result in anomalous TGCs and an enhancement in the production cross section as well as modifications to the shapes of kinematic distributions, such as the W and Z bosons transverse momenta. Because the Fermilab Tevatron is the only particle accelerator that can produce the charged state $WZ + X$, this measurement provides a unique opportunity to study the WWZ TGCs without any assumption on the values of the $WW\gamma$ couplings. Measurements of TGCs using the WW final state [4–8] are sensitive to both the $WW\gamma$ and WWZ couplings at the same time and must make some assumption as to how they are related to each other.

WZ production measurements and studies of WWZ couplings have been presented previously. The D0 Collaboration measured $\sigma_{WZ} = 4.5^{+3.8}_{-2.6}$ pb, with a 95% C.L. upper limit of 13.3 pb, using 0.3 fb^{-1} of $p\bar{p}$ collisions at $\sqrt{s} = 1.96$ TeV [9]. The observed number of candidates was used to derive the most restrictive available limits on anomalous WWZ couplings. More recently, the CDF Collaboration measured $\sigma_{WZ} = 5.0^{+1.8}_{-1.6}$ pb using 1.1 fb^{-1} of $p\bar{p}$ collisions at $\sqrt{s} = 1.96$ TeV [10], but did not present any results on WWZ couplings.

This communication describes a significant improvement to the previous D0 analysis. Not only is the data sample more than 3 times larger, but an improved technique is used to constrain the WWZ couplings. Instead of merely the total number of observed events, the number and the p_T distribution of the Z bosons (p_T^Z) produced in the collisions are compared to the expectations of non-SM WWZ couplings, significantly increasing the power of the WWZ coupling measurement over previous measurements [5,9].

We search for WZ candidate events in final states with three charged leptons, referred to as trileptons, produced when $Z \to \ell^+\ell^-$ and $W \to \ell'\nu$, where ℓ and ℓ' are $e^\pm$ or $\mu^\pm$. SM backgrounds can be suppressed by requiring three isolated high-p_T leptons and large missing transverse energy ($\not\!\!E_T$) from the neutrino. The combined branching fraction for these four possible final states (eee, $ee\mu$, $\mu\mu e$ and $\mu\mu\mu$) is 1.5% [11].

D0 is a multipurpose detector [12] composed of several subdetectors and a fast triggering system. At the center of the detector is a central tracking system, consisting of a silicon microstrip tracker (SMT) and a central fiber tracker (CFT), both located within a 2 T superconducting solenoidal magnet. These detectors are optimized for tracking and vertexing at pseudorapidities [13] $|\eta| < 3$ and $|\eta| < 2.5$, respectively. The liquid-argon and uranium calorimeter has a central section (CC) covering $|\eta| < 1.1$, and two end calorimeters (EC) that extend coverage to $|\eta| \approx 4.2$, with all three housed in separate cryostats [14]. An outer muon system, covering $|\eta| < 2$, consists of a layer of tracking detectors and scintillation trigger counters in front of 1.8 T iron toroids, followed by two similar layers after the toroids [15].

Electrons are identified by their distinctive pattern of energy deposits in the calorimeter and by the presence of a track in the central tracker that can be extrapolated from the interaction vertex to a cluster of energy in the calorimeter. Electrons measured in the CC (EC) must have $|\eta| < 1.1$ $(1.5 < |\eta| < 2.5)$. Electrons must have transverse energy $E_T > 15$ GeV and be isolated from other energy clusters. A likelihood variable, formed from the quality of the electron track and its spatial and momentum match to the calorimeter cluster and the calorimeter cluster information, is used to discrim-

inate electron candidates from instrumental backgrounds.

Muons tracks are reconstructed using information from the muon drift chambers and scintillation detectors and must have a matching central track with $p_T > 15$ GeV/c. Candidate muons are required to be isolated in the calorimeter and tracker to minimize the contribution of muons originating from jets [16].

Events collected from 2002–2006 using single muon, single electron, di-electron, and jet triggers were used for signal and background studies. The integrated luminosities [17] for the eee, $ee\mu$, $\mu\mu e$, and $\mu\mu\mu$ final states are 1070 pb^{-1}, 1020 pb^{-1}, 944 pb^{-1}, and 944 pb^{-1}, respectively. There is a common 6.1% systematic uncertainty on the integrated luminosities.

The WZ event selection requires three reconstructed, well-isolated leptons with $p_T > 15$ GeV/c. All three leptons must be associated with isolated tracks that originate from the same collision point and must satisfy the electron or muon identification criteria outlined above. To select Z bosons, and further suppress background, the invariant mass of a like-flavor lepton pair must fall within the range 71 to 111 GeV/c^2 for $Z \to ee$ events, and 50 to 130 GeV/c^2 for $Z \to \mu\mu$ events, with the mass ranges set by the mass resolution. For eee and $\mu\mu\mu$ decay channels, the lepton pair with invariant mass closest to that of the Z boson mass are chosen to define the Z boson daughter particles. The $\not\!\!E_T$ is required to be greater than 20 GeV, consistent with the decay of a W boson. The transverse recoil of the WZ system, calculated using the vector sum of the transverse momenta of the charged leptons and missing transverse energy, is required to be less than 50 GeV/c. This selection reduces the background contribution from $t\bar{t}$ production to a negligible level.

WZ event detection efficiencies are determined for each of the four final states. Monte Carlo (MC) events are generated using PYTHIA [18] and a GEANT [19] detector simulation and then processed using the same reconstruction chain as the data. Lepton identification efficiencies are determined from study of Z bosons in the D0 data. The average efficiencies for detecting an electron or muon with $E_T(p_T) > 15$ GeV are $(91 \pm 2)\%$ and $(90 \pm 2)\%$, respectively. The trigger efficiency for events with two (or more) electrons is estimated to be $(99 \pm 1)\%$. For events with two or three muons, the trigger efficiencies are estimated to be

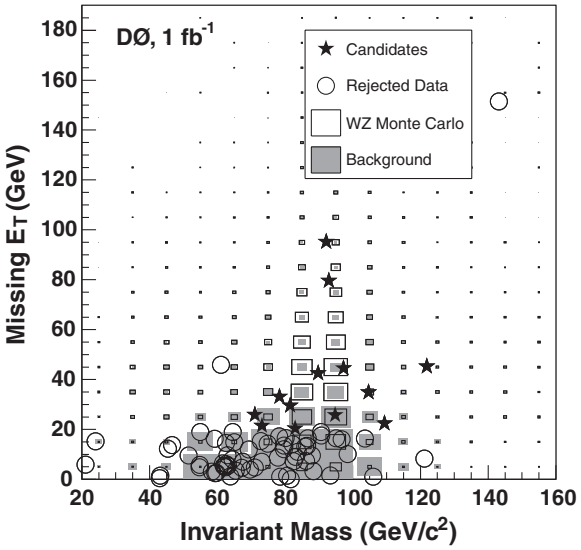

FIG. 1. $\not\!\!E_T$ versus dilepton invariant mass of WZ candidate events. The open boxes represent the expected WZ signal. The gray boxes represent the sum of the estimated backgrounds. The black stars are the data that survive all selection criteria. The open circles are data that fail either the dilepton invariant mass criterion or have $\not\!\!E_T < 20$ GeV.

$(91 \pm 5)\%$ and $(98 \pm 2)\%$, respectively. The kinematic and geometric acceptances range from 29% for the eee decay mode to 45% for the $\mu\mu\mu$ decay mode. It is also necessary to account for $\tau \to e, \mu$ final states of WZ that contribute to the signal. The number of τ events expected to satisfy the selection criteria is 0.67 ± 0.11 events. These are treated as signal in the cross section analysis, but are treated as background in the TGC analysis. Table I summarizes the efficiency determinations.

A total of 13 WZ candidate events is found. Figure 1 shows $\not\!\!E_T$ versus the dilepton invariant mass for the background, the expected WZ signal, and the data, including the candidates. Table I also details the number of candidates in each channel.

The main background for $WZ \to \ell' \nu_{\ell'} \ell \bar{\ell}$ are $Z + X$ events where X is a jet that has been misidentified as an electron or muon. We assess the background from Z + jets production by using an inclusive jet data sample that is selected with an independent jet trigger. Events characteristic of QCD two-jet production are used to measure the probability, as a function of jet E_T and η, that a single jet

TABLE I. The numbers of candidate events, expected signal events, and estimated background events, and the overall detection efficiency for the four final states.

Final state	Number of candidate events	Expected signal events	Estimated background events	Overall efficiency
eee	2	2.3 ± 0.2	1.2 ± 0.1	0.16 ± 0.02
$ee\mu$	1	2.2 ± 0.2	0.46 ± 0.03	0.17 ± 0.02
$\mu\mu e$	8	2.2 ± 0.3	2.0 ± 0.4	0.17 ± 0.03
$\mu\mu\mu$	2	2.5 ± 0.4	0.86 ± 0.06	0.21 ± 0.03
Total	13	9.2 ± 1.0	4.5 ± 0.6	—

will be misidentified as a muon or electron. Next, subsamples of ee + jets, $e\mu$ + jets, and $\mu\mu$ + jets events are selected using the same criteria as for the WZ signal except that the requirements for a third lepton in the event are dropped. The single jet-lepton misidentification probabilities are then convoluted with the measured jet distributions in the dilepton + jets subsamples to provide an estimate of the background from Z + jets events. The contribution for all four decay modes totals 1.3 ± 0.1 events.

All other backgrounds are determined using MC. Non-negligible backgrounds include SM ZZ production, $Z\gamma$ production, and W^*Z, WZ^*, or $W\gamma^*$ production. We define these processes as three-lepton final states produced through the decay of one on-mass-shell and one off-shell vector boson. These backgrounds and their determination are described in the following paragraphs.

ZZ production becomes a background when both Z bosons decay to charged leptons and one of the final state leptons escapes detection, thus mimicking a neutrino. The total contribution from ZZ production is 0.70 ± 0.08 events.

$Z\gamma$ final states can be misidentified as WZ events if the photon is misreconstructed as an electron and there is sufficient $\not\!\!E_T$. We estimate the $\ell\bar{\ell} + \gamma$ contribution using $Z + \gamma$ MC [20] combined with the probability for a photon to be misidentified as an electron ($4.2 \pm 1.5\%$) determined from studies of events with photons. This process is a background only to the eee and $\mu\mu e$ final states. The total contribution is 1.4 ± 0.5 events.

The contribution to the background from off-shell bosons should be nearly the same as occurs in similar processes and a fraction relative to the expected signal is determined from ZZ MC events generated using PYTHIA. It depends on the decay channel and varies from 8% for the $ee\mu$ mode to 15% for the $\mu\mu\mu$ mode. The uncertainties include all of those used for the signal plus an additional 16% systematic component to account for uncertainties in the off-shell component of the MC. The total contribution of this background is 0.99 ± 0.19 events.

To cross check the background estimates, we compare the number of observed events with that expected when we do not apply the dilepton invariant mass selection and the $\not\!\!E_T$ selection. We expected to observe 12.5 ± 1.4 events from signal and 62.9 ± 8.4 events from backgrounds. We observe the 78 events shown in Fig. 1.

The SM predicts that 9.2 ± 1.0 WZ events are expected to be observed in the data sample. The probability for the background, 4.5 ± 0.6 events, to fluctuate to 13 or more events is 1.2×10^{-3}, which translates to a one-sided Gaussian significance of 3.0σ, determined by using a Poisson distribution for the number of observed events in each channel convoluted with a Gaussian to model the systematic uncertainty on the background. A likelihood method [21] taking into account correlations among systematic uncertainties is used to determine the most probable WZ cross section. The cross section $\sigma(WZ)$ is $2.7^{+1.7}_{-1.3}$ pb, where the $\pm 1\sigma$ uncertainties are the 68% C.L. limits from the minimum of the negative log likelihood. The uncertainty is dominated by the statistics of the number of observed events.

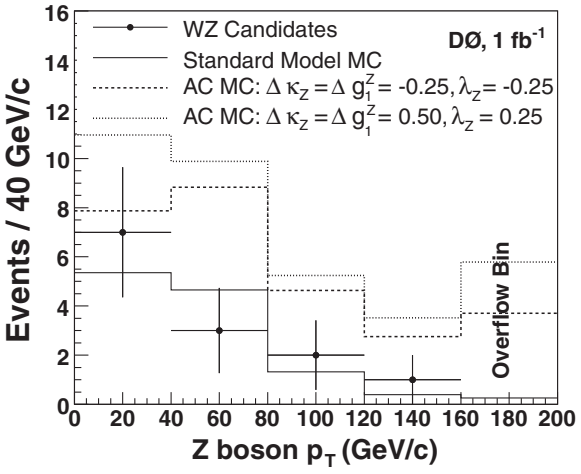

FIG. 2. The reconstructed Z boson p_T of the WZ candidate events used in the WWZ coupling parameter limit setting procedure. The solid histogram is the expected sum of signal and background for the case of the WWZ coupling parameters set to their SM values. The dotted and double dotted histograms are the expected sums of signal and background for two different cases of anomalous WWZ coupling parameter values. The black dots are the data. The final bin is the overflow bin.

By comparing the measured cross section and p_T^Z distribution to models with anomalous TGCs, we set one- and two-dimensional limits on the three CP-conserving coupling parameters. A comparison of the observed Z boson p_T distribution with MC predictions is shown in Fig. 2. We use the Hagiwara-Woodside-Zeppenfeld (HWZ) [22] leading-order event generator processed with a fast detector and event reconstruction simulation to produce events with anomalous WWZ couplings and simulate their efficiencies and acceptances. The HWZ event generator does not account for τ final states, and as a result, we treat the 0.7 event τ contribution as background for the WWZ coupling limit setting procedure. The method used to determine the coupling limits is described in Ref. [23]. Limits are set on the coupling parameters λ_Z, Δg_1^Z, and

TABLE II. One-dimensional 95% C.L. intervals on λ_Z, Δg_1^Z, and $\Delta\kappa_Z$ for two sets of form factor scale, Λ.

$\Lambda = 1.5$ TeV	$\Lambda = 2.0$ TeV
$-0.18 < \lambda_Z < 0.22$	$-0.17 < \lambda_Z < 0.21$
$-0.15 < \Delta g_1^Z < 0.35$	$-0.14 < \Delta g_1^Z < 0.34$
$-0.14 < \Delta\kappa_Z = \Delta g_1^Z < 0.31$	$-0.12 < \Delta\kappa_Z = \Delta g_1^Z < 0.29$

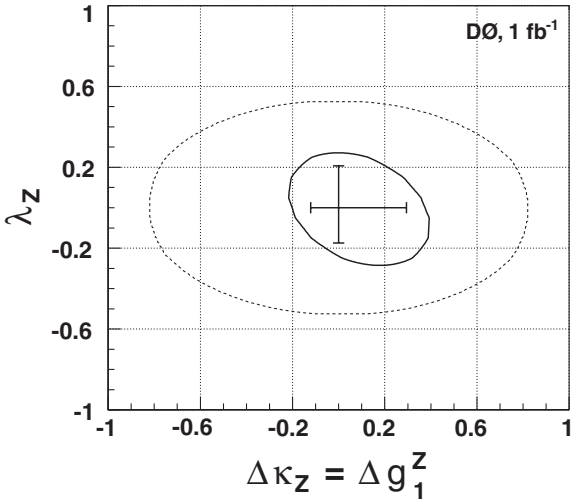

FIG. 3. Two-dimensional 95% C.L. contour limit in $\Delta g_1^Z = \Delta\kappa_Z$ versus $\Delta\lambda_Z$ space (inner contour). The form factor scale for this contour is $\Lambda = 2$ TeV. The physically allowed region (unitarity limit) is bounded by the outer contour. The cross hairs are the 95% C.L. one-dimensional limits.

$\Delta\kappa_Z$. Two-dimensional grids are constructed in which the parameters λ_Z and Δg_1^Z are allowed to vary simultaneously. Table II presents the one-dimensional 95% C.L. limits on λ_Z, Δg_1^Z and $\Delta\kappa_Z$. Figure 3 presents the two-dimensional 95% C.L. limits under the assumption $\Delta g_1^Z = \Delta\kappa_Z$ [3] for $\Lambda = 2$ TeV. The form factor scale, Λ [24], associated with each grid, is chosen such that the limits are within the unitarity bound.

In summary, we present the results of a search for WZ production in 1.0 fb^{-1} of $p\bar{p}$ collisions at $\sqrt{s} = 1.96$ TeV. We observe 13 trilepton candidate events with an expected 9.2 ± 1.0 signal events and 4.5 ± 0.6 events from background. This gives an observed significance of 3.0σ. We measure the WZ production cross section to be $2.7^{+1.7}_{-1.3}$ pb, in agreement with the SM prediction. We use the measured cross section and p_T^Z distribution to improve constraints on WWZ trilinear gauge couplings by a factor of 2 over the previous best results.

We thank the staffs at Fermilab and collaborating institutions, and acknowledge support from the DOE and NSF (USA); CEA and CNRS/IN2P3 (France); FASI, Rosatom and RFBR (Russia); CAPES, CNPq, FAPERJ, FAPESP and FUNDUNESP (Brazil); DAE and DST (India); Colciencias (Colombia); CONACyT (Mexico); KRF and KOSEF (Korea); CONICET and UBACyT (Argentina); FOM (The Netherlands); Science and Technology Facilities Council (United Kingdom); MSMT and GACR (Czech Republic); CRC Program, CFI, NSERC and WestGrid Project (Canada); BMBF and DFG (Germany); SFI (Ireland); The Swedish Research Council (Sweden); CAS and CNSF (China); Alexander von Humboldt Foundation; and the Marie Curie Program.

[1] J. M. Campbell and R. K. Ellis, Phys. Rev. D **60**, 113006 (1999).
[2] K. Hagiwara, R. D. Peccei, D. Zeppenfeld, and K. Hikasa, Nucl. Phys. **B282**, 253 (1987).
[3] K. Hagiwara, S. Ishihara, R. Szalapski, and D. Zeppenfeld, Phys. Rev. D **48**, 2182 (1993). The authors parameterize the WWZ couplings in terms of the $WW\gamma$ couplings: $\Delta\kappa_Z = \Delta\kappa_\gamma(1 - \tan^2\theta_W)/2$, $\Delta g_1^Z = \Delta\kappa_\gamma/(2\cos^2\theta_W)$ and $\lambda_Z = \lambda_\gamma$.
[4] F. Abe *et al.* (CDF Collaboration), Phys. Rev. Lett. **78**, 4536 (1997).
[5] B. Abbott *et al.* (D0 Collaboration), Phys. Rev. D **60**, 072002 (1999). This report contains both a description of a search for $WZ \rightarrow$ trileptons with anomalous WWZ coupling limits and a search for non-standard-model $WW + WZ \rightarrow \ell\nu$jet jet production with limits on anomalous $WW\gamma$ and WWZ couplings.
[6] LEP Collaborations ALEPH, DELPHI, L3, OPAL, and LEP TGC Working Group, Report No. LEPWWG/TGC/2005-01, 2005. The authors parameterize WWZ couplings in terms of the $WW\gamma$ couplings: $\Delta\kappa_Z = \Delta g_1^Z - \Delta\kappa_\gamma \tan^2\theta_W$ and $\lambda_Z = \lambda_\gamma$.
[7] V. M. Abazov *et al.* (D0 Collaboration), Phys. Rev. D **74**, 057101 (2006).
[8] T. Aaltonen *et al.* (CDF Collaboration), arXiv:0705.2247.
[9] V. M. Abazov *et al.* (D0 Collaboration), Phys. Rev. Lett. **95**, 141802 (2005).
[10] A. Abulencia *et al.* (CDF Collaboration), Phys. Rev. Lett. **98**, 161801 (2007).
[11] W.-M. Yao *et al.* (Particle Data Group), J. Phys. G **33**, 1 (2006).
[12] V. M. Abazov *et al.* (D0 Collaboration), Nucl. Instrum. Methods Phys. Res., Sect. A **565**, 463 (2006).
[13] The D0 coordinate system is cylindrical with the z-axis along the proton beamline and the polar and azimuthal angles denoted as θ and ϕ respectively. The pseudorapidity is defined as $\eta = -\ln\tan\theta/2$.
[14] S. Abachi *et al.* (D0 Collaboration), Nucl. Instrum. Methods Phys. Res., Sect. A **338**, 185 (1994).
[15] V. Abazov *et al.*, Nucl. Instrum. Methods Phys. Res., Sect. A **552**, 372 (2005).
[16] V. Abazov *et al.*, Phys. Rev. D **76**, 052006 (2007).
[17] T. Andeen *et al.*, Report No. FERMILAB-TM-2365, 2007.
[18] T. Sjöstrand *et al.*, Comput. Phys. Commun. **135**, 238 (2001).
[19] R. Brun *et al.*, Report No. CERN-DD-78-2-REV, 1994 (unpublished).
[20] U. Baur and E. L. Berger, Phys. Rev. D **41**, 1476 (1990).

[21] G. J. Feldman and R. D. Cousins, Phys. Rev. D **57**, 3873 (1998).

[22] K. Hagiwara, J. Woodside, and D. Zeppenfeld, Phys. Rev. D **41**, 2113 (1990).

[23] V. M. Abazov *et al.* (D0 Collaboration), Phys. Rev. Lett. **94**, 151801 (2005).

[24] U. Baur, arXiv:hep-ph/9510265.